International Global Navigation Satellite Systems Association
IGNSS Conference 2016

Colombo Theatres, Kensington Campus, UNSW Australia
6 – 8 December 2016

Evaluation of accuracy, integrity and availability of ARNS multi-constellation signals for aviation users in Australia

Manoj Deo
PhD Candidate, Department of Spatial Sciences, Curtin University,
GPO Box U 1987, Perth WA 6845, Australia
Phone: +61 432163000
Email: manoj.deo01@gmail.com

Ahmed El-Mowafy
Assoc. Professor, Department of Spatial Sciences, Curtin University,
GPO Box U 1987, Perth WA 6845, Australia
Phone: +61 8 9266 3403
Fax: +61 8 9266 2703
Email: a.el-mowafy@curtin.edu.au

ABSTRACT

Aviation requires the use of signals operating in the protected aeronautical radionavigation service (ARNS) band. For GPS, only single frequency signal (L1 C/A) are currently allowed, which contains ionosphere delays. Although Space Based Augmentation Systems (SBAS) may be used to enhance the accuracy and integrity of single frequency aviation users, this service is not available in Australia. GPS Block IIF satellites transmitting the L5 civil signal, which falls in the ARNS band allows for elimination of ionospheric delay when combined with L1 C/A. Beidou has two ARNS protected signals, whereas Galileo has three protected signals. With these systems, multi-frequency multi-constellation (MFMC) GNSS may become a primary means of navigation in the next decade for all phases of flight operations, including precision approach.

This paper presents the current status of the accuracy, integrity and availability of ARNS protected signals in Australia which will help in early understanding of its future performance. The present number of MFMC satellites in operation can facilitate this initial testing. MFMC data for ARNS signals collected from several Australian sites was analysed to demonstrate the current snapshot of accuracy, availability and integrity for aviation. Promising results are shown and further improvements are expected as additional satellites are launched, with improved information. Analysis of integrity monitoring with tested MFMC data showed that integrity can be achieved for almost 100% of the time.

KEYWORDS: GNSS, positioning, navigation, accuracy, availability.

1. INTRODUCTION

The uptake of GPS navigation in commercial aviation has been ever increasing since it achieved full operational capability. GPS is the fundamental enabling technology for several aviation navigation services such as surveillance monitoring with Automatic Dependent Surveillance-Broadcast (ADS-B), Performance Based Navigation (PBN), Ground Based Augmentation System (GBAS), Space Based Augmentation System (SBAS), Localiser Performance with Vertical guidance (LPV), and Advanced Receiver Autonomous Integrity Monitoring (ARAIM). The civil aviation order (20.18) issued by the Civil Aviation Services Australia (CASA) has mandated Global Navigation Satellite Systems (GNSS) as the primary means of navigation for all Instrument Flight Rule (IFR) aircraft in the Australia from 4 February 2016 (CASA, 2013).

Australia is in a GNSS hotspot, where in addition to the global systems (GPS, Galileo, Beidou and GLONASS), it has access to main regional navigation satellite systems such as QZSS and NAVIC. Beidou, which is expected to have global coverage by 2020, has full operational capability over most of Australia. Along with the multi-constellation systems, aviation users now have access to multi-frequency signals that are protected within the designated safety-of-life aeronautical radionavigation service (ARNS) band, which allows for removal of first order ionospheric errors. In addition to L1 C/A, GPS at the time of writing has 12 Block IIF satellites in operation, which transmit an extra ARNS signal, L5. Beidou has 20 satellites with two ARNS signals, namely B1 and B2; whereas Galileo has 12 satellites with three ARNS signals, namely E1, E5a and E5b. At present, the GPS L5 signal is considered pre-operational, implying that the availability and performance of the signal may not comply with all requirements of the interface specifications; hence its usage is at user's own risk (NANU message 2014039). The use of Beidou and Galileo signals in aviation is yet to be regulated by the International Civil Aviation Organisation (ICAO). However, the Radio Technical Commission for Aeronautics (RTCA) is developing Minimum Operational Performance Standards (MOPS) for Multi Frequency Multi-constellation (MFMC) receivers tracking GPS L1/L5, Galileo, GLONASS and Beidou ARNS signals, which is expected to be released in 2018 (RTCA, 2014).

Given these developments in GNSS procedures for aviation, this paper analyses the present status of the accuracy and availability of ARNS protected signals in Australia as an indication of the expected future performance. A new low noise, triple frequency ionosphere-free linear combination of the Galileo E1-E5a-E5b and the dual frequency GPS L1-L5 and Beidou B1-B2 ionosphere-free combinations are used to improve accuracy and continuity/ availability. MFMC data from GPS, Galileo and Beidou constellations for ARNS protected signals at six Australian sites is analysed to determine positioning accuracy, availability and integrity. The availability is measured in terms of the percentage of time when the minimum number and geometry of satellites required to obtain the desired performance-based positioning are available. Satellite geometry is measured through the Dilution of Position (DOP) parameters. Accuracy is analysed by comparing computed positions to the precisely known coordinates of the stations. A brief analysis of integrity monitoring is also presented, and readers may refer to more thorough analysis in the Australian context in El-Mowafy (2016) and El-Mowafy & Yang (2016). Since the ionosphere-free combination of ARNS signals for GPS and Galileo is not the standard combination used to generate satellite clock corrections, it is thus shown that the Differential Code Biases (DCBs) must be applied to get the best accuracy in the height component. The commonly used antenna Phase Centre Offsets (PCO) for Beidou differ significantly from recently calibrated values for selected satellites. Thus, provision of improved calibrated PCO values, as well as additional launches of ARNS satellites may meet the LPV-200 positional accuracy requirements for future aviation users in Australia.

The next section summarises the application of GNSS for navigation in aviation, followed by a description of GNSS observation models used, description of the analysis methodology and error modelling of DCBs, antenna phase centre offsets and troposphere delay. Results analysing accuracy and integrity are presented for six GNSS continuous operating stations in Australia, followed by conclusions.

2. GNSS NAVIGATION IN AVIATION

This section provides a brief summary of the present day use of GNSS for navigation in aviation.

2.1 Automatic Dependent Surveillance Broadcast (ADS-B)

ADS-B enables an aircraft to transmit its GPS determined position to air traffic control (ATC) via a ground communication link, such that the position is displayed on ATC consoles in real time. It also allows positions of surrounding aircraft to be displayed on the pilot's cockpit screen, thus enabling situational awareness of traffic. ADS-B has numerous advantages over commonly used radar surveillance technology, such as lower installation and maintenance costs, greater coverage and improved accuracy. Under Civil Aviation Order 20.18 effective on 2 February 2017, ABS-B transmitting equipment will be mandatory for all aircraft operating under IFR (CASA, 2013).

2.2 Performance Based Navigation (PBN)

PBN covers two specifications; area navigation (RNAV) and Required Navigation Performance (RNP), both of which have been endorsed by ICAO. RNAV allows navigation of an aircraft along its flight path with the aid of space based navaids and has been used in Australia since 1995. The CASA mandate for GNSS as the primary means of navigation has led to a significant reduction in the ground based navaid network such as Distance Measuring Equipment (DME), Non-directional Beacons (NDB) and VHF Omni Directional Radio Range (VOR) (Hannan, 2015).

RNP requires equipment based navigation as well as performance monitoring of navigation accuracy and integrity on board the aircraft. Integrity is the ability of a system to detect and exclude faults and provide timely warnings as to when not to use the system for navigation (El-Mowafy, 2013); and the trustworthiness of a position solution from a system, provided in a timely manner to users, with a certain probability (Speidel et al, 2013). When using RNP, the integrity of the aircraft position is derived from Receiver Autonomous Integrity Monitoring (RAIM) algorithms on board the aircraft receiver. A RNP of 0.1 requires the aircraft position with an accuracy such that the Total System Error (TSE) is better than 0.1 nautical miles (NM) for more than 95% of the flight time. Performance monitoring is done using Receiver Autonomous Integrity Monitoring (RAIM) algorithms and an alert is issued if the algorithm detects that the probability of the TSE exceeding $2 \times 0.1NM$ is greater than 0.99999. In such case the flight crew is alerted and the pilot may take necessary steps to abort the RNP procedure. This becomes critical when attempting to land during poor weather conditions in undulating terrain. RNP allows aircraft to fly precisely along predictable and repeatable flight paths, avoid airborne holding, flight diversions, or even cancellations (ATAG, 2013). RNP also enables curved approach paths with reduced flight distance (hence reduced fuel consumption and CO_2 emissions) and permits aircraft to fly safely at closer separation distance.

2.3 Space Based Augmentation Systems (SBAS) and Ground Based Augmentation System (GBAS)

SBAS and GBAS technologies enable timely provision of correction and integrity information to aviation users in real-time. SBAS provides regional based corrections to atmospheric, satellite orbit and clock errors as well as integrity messages transmitted from geostationary satellites. These corrections are based on a ground network of aviation specific Continuously Operating reference Stations (CORS) tracking GNSS measurements. Several SBAS are in operation at present such as the European EGNOS, USA Wide Area Augmentation System (WAAS), Japanese MSAS and the Indian NAVIC. Apart from aviation, SBAS users include other applications requiring metre level accuracy such as marine, agriculture and autonomous vehicle navigation. According to a recent economic study, the cost of implementing SBAS in Australia could outweigh the benefits (Allen Consortium, 2013), thus it is not planned yet.

In aviation, GBAS (with its US implementation also known as Local Area Augmentation System (LAAS)), comprises of a mini-network of ground sensors, usually within the airport premises, monitors GPS signals and transmits, corrections and integrity messages to aircraft but within a few tens of nautical miles from the airport. For example the GBAS implementation in Sydney airport is certified with an operational radius of 23NM surrounding the aerodrome. A GBAS Landing System (GLS) improves airport resilience, runway capacity and predictability of arriving traffic (Guillermet, 2016). Compared to an Instrument Landing System (ILS), it serves multiple runways rather than a single system per runway end and is practically equivalent to a Category I (CAT I) approach with the same level of safety. However, the GLS service is limited to a small coverage radius of a few tens of NM, and requires compatible avionics on board the aircraft in order to attempt GLS approaches. Research is underway to gain regulatory certification of GLS for CAT II/ III minima by the end of this decade. CAT II/ III approaches maintain safety when landing in low visibility Instrument Meteorological Conditions (IMC), thus increasing airport capacity.

2.4 Advanced RAIM (ARAIM)

In the past few years, ARAIM algorithms have been proposed as an evolution of traditional RAIM to monitor the integrity of vertical and horizontal positioning for more demanding phase of flight. ARAIM provides the confidence that possible vertical error is bounded by a Vertical Protection Level (VPL) VPL, and an alert is issued if this exceeds a prescribed threshold Vertical Alert Limit (VAL). The ARAIM algorithm is currently targeted for Localizer Performance with Vertical guidance with a decision height (DH) of 200 feet above the runway, referred to as LPV-200. The positioning and integrity requirements of the LPV-200 approach procedure is close to the CAT I performance achieved from ILS or GLS. Table 1 compares the performance requirements for LPV-200, CAT I/ II/ III to other approach procedures for landing civil aircraft including Non Precision Approach (NPA), Approach with Vertical Guidance (APV) and Lateral/ Vertical Navigation (LNAV/ VNAV) (Speidel et al, 2013; ICAO, 2007).

Aircraft Phase of Flight	**Accuracy**		**Integrity**			**Maximum Probabilities of Failure**	
	2σ *or* 95%		Alert Limits		Time to Alert	Integrity	Continuity
	Vertical	Horizontal	Vertical	Horizontal			
NPA, Initial Approach, Departure	N/A	0.22–0.74km	N/A	1.95–3.7km	10–15 s	$10^{-7}/\,hr$	$10^{-4}/hr$
LNAV/ VNAV	20m	220m	50m	556m	10 s	$1.2 \times 10^{-7}/150\ s$	$4.8 \times 10^{-4}/15\ s$
LPV		16m		40m			
APV I			35m				
APV II	8m		20m		6 s		
LPV-200	4m		35m				
Precision Approach CAT I			10m				
Precision Approach CAT II/ III	< 2.9m	< 6.9m	5.3m	< 17m	< 2s	$< 10^{-9}/150\ s$	$< 4 \times 10^{-6}/15s$

Table 1: Performance requirements for landing civil aircraft (source: Speidel et al., 2013).

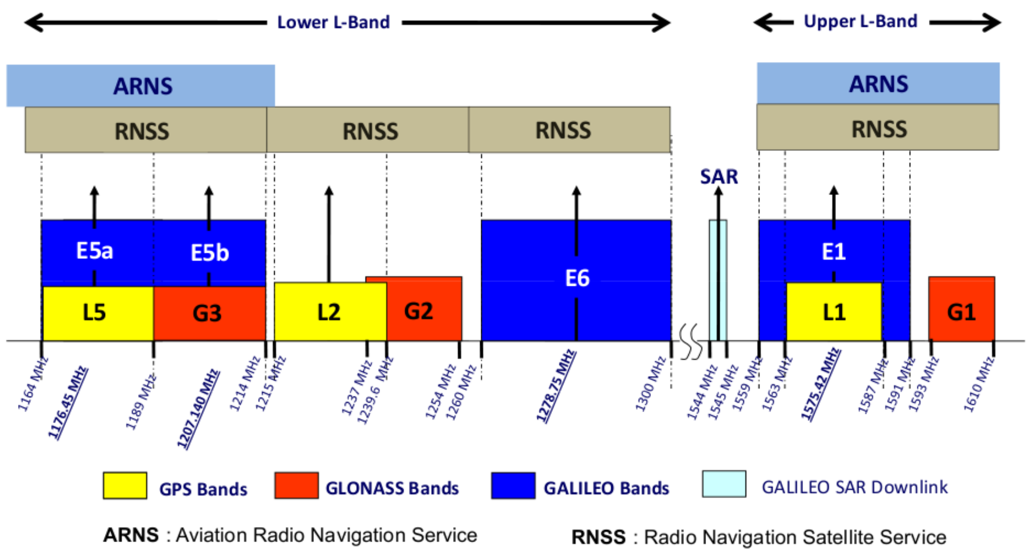

Figure 1: GNSS signal frequencies in the ARNS protected band. (Source: (*http://www.navipedia.net/index.php/GNSS_signal*)

3. GNSS OBSERVATION MODEL

The observation equation of the pseudorange code measurements for satellite o from one GNSS constellation such as GPS (denoted as G) on frequency i in length units can be formulated as follows:

$$P_i^{o_G} = \rho^{o_G} + c\left(dt_G - dt^{o_G} + d_{i_G} - d_i^{o_G}\right) + T^{o_G} + \mu_i I^{o_G} + \varepsilon_{P_i}^{o_G} \qquad (1)$$

where $P_i^{o_G}$ is the code measurement from system G, ρ^{o_G} is the satellite-to-receiver geometric range, c is the speed of light in vacuum; dt_{G} and dt^{o_G} are the receiver and satellite clock offsets; $d_{i_{\mathrm{G}}}$ and $d_i{}^{o_G}$ are the receiver and satellite hardware biases in time units, respectively; T^{o_G} is the tropospheric delay, $\mu_i = \frac{f_1^2}{f_i^2}$ is the dispersive coefficient of the ionosphere, I^{o_G} is the ionosphere error for the L1 reference frequency; $\varepsilon_{Pi}^{o_G}$ comprises code measurement noise and multipath.

For the Beidou constellation (denoted as C) with frequency j from satellite p, the pseudorange code measurement is:

$$P_j^{p_C} = \rho^{p_C} + c\left(dt_C - dt^{p_C} + d_{j_C} - d_j{}^{p_C}\right) + T^{p_C} + \mu_j I^{p_C} + ISTB_{G-C} + \varepsilon_{P_j}^{p_C} \tag{2}$$

The terms are similar to the ones described for system G above, but apply to satellite p on system C and signal j. $ISTB_{G-C}$ is the inter-system time bias between systems G and C (i.e. GPS and Beidou), combined for the receiver and the satellite. Similar equation is derived for the Galileo constellation (denoted as E). When integrating data from multiple constellations, users have to consider the differences in coordinate frames, particularly when using broadcast orbits. When using the precise orbits from International GNSS Service (IGS) or its subordinate Multi-GNSS Experiment (M-GEX), the orbits for all constellations are consistent with ITRF.

4. ERROR TREATMENT IN MFMC OBSERVATION

This section describes the different corrections applied in our study to reduce positioning errors for aviation users of MFMC data from GPS, Beidou and Galileo.

4.1 Ionosphere-free Combinations

To eliminate the first order ionosphere delay, the dual frequency ionosphere-free combination of the ARNS signals is used for GPS and Beidou, respectively, as follows:

$$P^{o_G} = \frac{f_{L1}^2}{f_{L1}^2 - f_{L5}^2} P_{L1}^{o_G} - \frac{f_{L5}^2}{f_{L1}^2 - f_{L5}^2} P_{L\%}^{o_G} = 2.260604 \cdot P_{L1}^{o_G} - 1.260604 \cdot P_{L5}^{o_G} \tag{3}$$

$$P^{p_C} = \frac{f_{B1}^2}{f_{B1}^2 - f_{B2}^2} P_{B1}^{p_C} - \frac{f_{B2}^2}{f_{B1}^2 - f_{B2}^2} P_{B2}^{p_C} = 2.487168 \cdot P_{B1}^{p_C} - 1.487168 \cdot P_{B2}^{p_C} \tag{4}$$

Since there are three signals on ARNS frequencies for Galileo (i.e. E1, E5a & E5b), a low noise triple frequency ionosphere-free combination developed in Deo and El-Mowafy (2016) is used as follows:

$$P^{q_E} = 2.314925 \cdot P_{E1}^{q_E} - 0.836269 \cdot P_{E5a}^{q_E} - 0.478656 \cdot P_{E5b}^{q_E} \tag{5}$$

4.2 Differential Code Biases (DCBs)

Single frequency GPS users apply the time group delay (TGD) parameter provided in the GPS navigation message, which represents a scaled version of the differential hardware biases in the satellite. Future navigation messages will also broadcast inter-signal corrections (ISCs) as part of the new civil navigation (CNAV) message of the L2C and L5 signals, as well as the CNAV-2 message data for the future L1C signal. These TGDs and ISCs are equivalent to the satellite Differential Code Biases (DCB), now provided daily by the IGS Multi-GNS Experiment (M-

GEX) (Montenbruck et al 2014). A procedure for estimation and transmission of DCB correction for GPS L1-L5 WAAS users is discussed in Grewal et al. (2008). This applies for the Geostationary (GEO) WAAS satellites transmitting L1 and L5, and will be available for GPS IIF and GPS III satellites when the constellation is complete. The DCB corrections must also be considered for Galileo and Beidou constellations, which will be broadcast to aviation users in the future. In the new methods such as ARAIM, ionosphere-free combination observations are used to mitigate the ionosphere delay. However, since these are not available at present, the IGS M-GEX DCBs are used in this paper only for demonstration purpose of its impact on positioning accuracy. DCBs for various code measurements and tracking combinations of GPS, Galileo and BeiDou observations, with daily repeatability of 0.05-0.3ns, are now provided daily by IGS M-GEX website at ftp://cddis.gsfc.nasa.gov/pub/gps/products/M-GEX/dcb. The DCB product generated by German Aerospace Centre (DLR) (Montenbruck et al., 2014) is used in this study.

4.3 Antenna Phase Centre Offset (PCO)

The GNSS signals are transmitted from the electrical phase centre of the satellite, whereas the satellite orbit positions are referenced to its Centre of Mass (CoM) (Dilssner et al., 2014). The difference between the mean phase centre and CoM is known as the Phase Centre Offset (PCO) and this must be applied to the computed satellite positions to tie to the origin of GNSS measurements. Users of the broadcast navigation orbit do not need to apply this correction since broadcast orbits are referenced to the satellite phase centre. The satellite absolute PCO corrections for GPS satellites are available in ANTEX format from the IGS ftp site https://igscb.jpl.nasa.gov/igscb/station/general/pcv_archive/. This file has the PCOs in a satellite specific coordinate system, as well as the Phase Centre Variations (PCV), which vary depending on the satellites nadir angle (Schmid et al., 2007). The PCOs are applicable for the L1-L2 ionosphere-free combination, and strictly speaking these are not applicable to the L1-L5 ionosphere-free combination used in aviation. However, in the absence of these data, the L1-L2 offsets are used in this study. An important point to consider when applying PCO correction is that a PRN sequence may have been assigned to several satellites for specific durations, although only one satellite transmits a PRN sequence at a point in time. Thus the user must select the PCO correction that is relevant for the PRN at the time of measurement, when analysing historical data.

For Galileo and BeiDou satellites, conventional phase centre offsets are recommended for use by IGS M-GEX (see http://igs.org/M-GEX/), which are summarised in Table 2 and apply for all frequencies. These PCOs are taken from satellite drawings and therefore can only give a rough estimate of the location of “true” phase center. Dilssner et al. (2014) determined these offsets using more than one year of Beidou measurements and for the B1-B2 ionosphere-free combination, the offsets were 0.549m in x-coordinate, and ranged from 3-4m for IGSO satellites and 2.0-2.4m for MEO satellites in z-coordinate. The calibrated z-coordinates (which is aligned with the geocenter, or bore-sight direction of the antenna) are vastly different from the IGS M-GEX recommended values, by as much as 3.9m.

The PCO is defined in a satellite-fixed right-handed coordinate system (Rothacher et al., 2010), must be converted to an Earth-Centred-Earth-Fixed (ECEF) coordinate system, such as ITRF2008, which requires the position of the Sun as well as the satellite, at the measurement time. The procedure for applying the PCO correction is described in Pajares-Hernandez (2011).

GNSS	PRNS	x-offset	y-offset	z-offset
Galileo IOV	E11, E12, E19, E20	-0.2	0.0	+0.6
Galileo FOC	E18, E14, E26, E22, E24, E30, E08, E09, E01, E02	+0.15	0.0	1.0
Beidou	All	+0.6	0.0	1.1

Table 2: IGS M-M-GEX recommended satellite Phase Centre Offsets for Galileo and Beidou satellites.

4.4 Troposphere Modelling

Tropospheric corrections are available for aviation users as part of integrity messages from SBAS systems such as the UNB3 troposphere model used in WAAS (Collins and Langley, 1999). Standard positioning algorithms for aviation ignores the troposphere, particularly the wet component of the delay. However, SBAS is not available in Australia and since tropospheric errors largely affect the height component (particularly close to ground where the aircraft approach takes place) it becomes critical to accurately model it in order to achieve LPV-200 requirements.

The tropospheric delay along the signal path $T(E)$ is modelled as (Tuka and El-Mowafy, 2013)

$$T(E) = ZHD \cdot m_h + ZWD \cdot m_w \tag{6}$$

Where E is the elevation angle of the satellite, ZHD, ZWD are the hydrostatic and wet delay components in zenith direction and m_h, m_w are the hydrostatic and wet mapping functions. The zenith hydrostatic delay can be calculated with the Saastamoinen's formula, given in Davis et al. (1985) as

$$ZHD = P \cdot \frac{0.00022768}{1-0.00266 \cdot cos(2\phi)-0.28 \cdot 10^{-6}h} \tag{7}$$

Where P is the atmospheric pressure ϕ is the station latitude and h is the station orthometric or ellipsoid height, the difference between using either height system is considered negligible (IERS Conventions, 2010).

Only approximate zenith wet delay can be calculated with measurements of relative humidity and temperature are available at the receiver as described in Andrei and Chen (2009):

$$ZWD = 0.002277 \left(\frac{1255.0}{Temp} + 0.05\right) 6.108 \frac{RH}{100} \cdot exp\left(\frac{17.15 \cdot Temp - 4684}{Temp - 38.45}\right) \tag{8}$$

Where RH is the relative humidity, $Temp$ is the temperature in Kelvin and e is the partial pressure of water vapour. Users should note that this method of computation is not appropriate for cm level positioning where accurate wet zenith delay requires knowledge of the vapour water content along the signal path, which is hard to be measured.

The pressure value, used in Eq. 7, may be computed from the Global Pressure Temperature (GPT) empirical model (Bohem, et al., 2007). However, use of GPT was found to be inadequate for precise positioning, resulting in pressure correlated height errors of 10mm, or higher for satellite elevation angles less than 10 degrees (Kouba, 2009). A refined empirical weather model, GPT2, was introduced in Lagler et al. (2013). GPT2 enables estimation of the total tropospheric delay as an improved alternative to the US Standard Atmosphere. GPT2 gives the pressure, temperature, temperature lapse rate, partial water vapour, as well the Vienna Mapping Function (VMF1) required parameters; hence both ZHD and ZWD may be calculated using Eq. 7 and 8. Since it gives VMF1 parameters, users no longer need to use the less accurate Global Mapping Function (GMF). Also, the GPT2 model parameters and may be stored inside the receiver memory for real-time computations as required in aviation.

5. TESTING

In this study, MFMC data for ARNS signals was obtained in RINEX V3.02 format for 14 April 2016, for six continuously operated (CORS) GNSS stations which are distributed Australia wide. This provides a test case for similar distribution and availability of satellites for aviation users. The test stations were the IGS M-GEX station CUT0 (Curtin University, Perth. Western Australia) and ARGN/ AuScope stations ALIC (Alice Springs, Northern Territory), NEBO (Nebo, Queensland), FLND (Flinders Island, Tasmania), TOW2 (Townsville, Queensland), and KARR (Karratha, Western Australia). Test results are presented in terms of accuracy, availability and integrity using the ARNS data applicable to aviation users. These results provide a current snapshot of the aviation performance and improvements are expected when the GNSS systems are fully operational.

5.1 Application of DCBs

As stated earlier, since the broadcast DCBs are unavailable for aviation users, the IGS M-GEX DCB biases are used to demonstrate its impact on positioning accuracy. Users should apply the DCB correction that is relevant for the tracking channel properties of the receiver, as per RINEX V3 notation. Figures 2(a) and (b) compare the position errors computed as the difference between the computed positions and the known point coordinates for station ALIC with and without DCB correction. As shown, the height component is significantly affected at the 0.3m level if DCBs are not applied. For this test case, the standard deviations (Std) in East, North and Up improved by 11.8%, 7.5% and 11.5%, respectively after applying DCB correction.

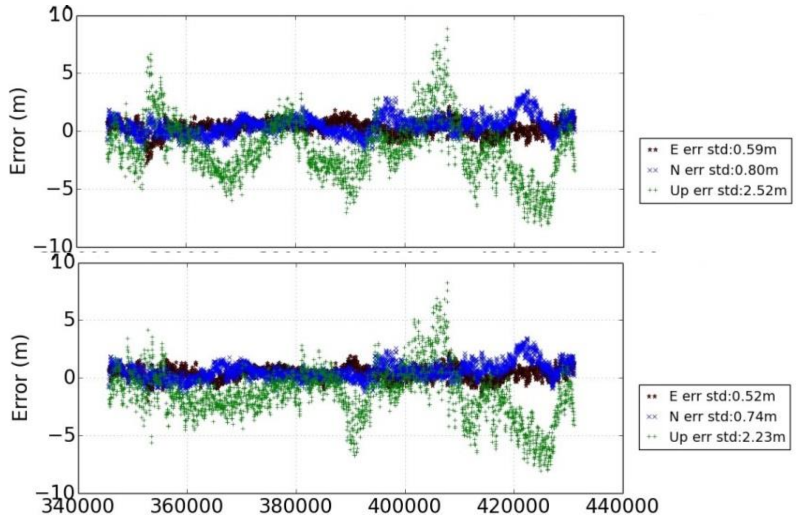

Figure 2: Positional error at station ALIC without DCB correction (top) and with DCB correction applied (bottom).

5.2 Accuracy and Availability Results

Figure 3 shows the positional error, satellite availability and geometry (DOPs) at station CUT0 during the observation period. Accuracy is analysed with respect to the precisely known coordinates of the stations, which were obtained from the Asia Pacific Reference Frame (APREF) solution for the observation week, i.e. GPS week 1892. Table 3 presents the standard deviation (Std) and root mean squared (RMS) of the Easting (E), Northing (N) and vertical (Vert) positional errors at each measurement epoch for each of the six stations. The positional accuracy at KARR and ALIC was better than most of the other stations, whereas TOW2 had the worst accuracy. The criteria for LPV-200 positional accuracy is clearly met for horizontal accuracy (2*Std = 16m) at all stations, but the vertical accuracy achieved falls short of the required accuracy (2 Std = 4m) on average by 0.5m.

Station	Std E	Std N	Std Hor	Std Vert	RMS E	RMS N	RMS Hor	RMS Vert
ALIC	0.52	0.74	0.58	2.23	0.65	0.93	1.13	2.64
CUT0	0.87	0.98	0.75	2.15	0.89	1.12	1.43	2.86
NEBO	0.86	0.81	0.73	2.29	0.97	1.13	1.49	2.33
FLND	0.69	0.95	0.88	2.26	0.88	1.68	1.90	2.30
TOW2	2.23	0.93	2.06	4.64	2.38	1.45	2.78	4.70
KARR	0.58	0.71	0.52	1.82	0.58	0.82	1.01	2.47

Table 3: Standard Deviation and RMS of positional error of with Multi-constellation ARNS data (GPS+Galileo+Beidou). All values are in units of metres (m).

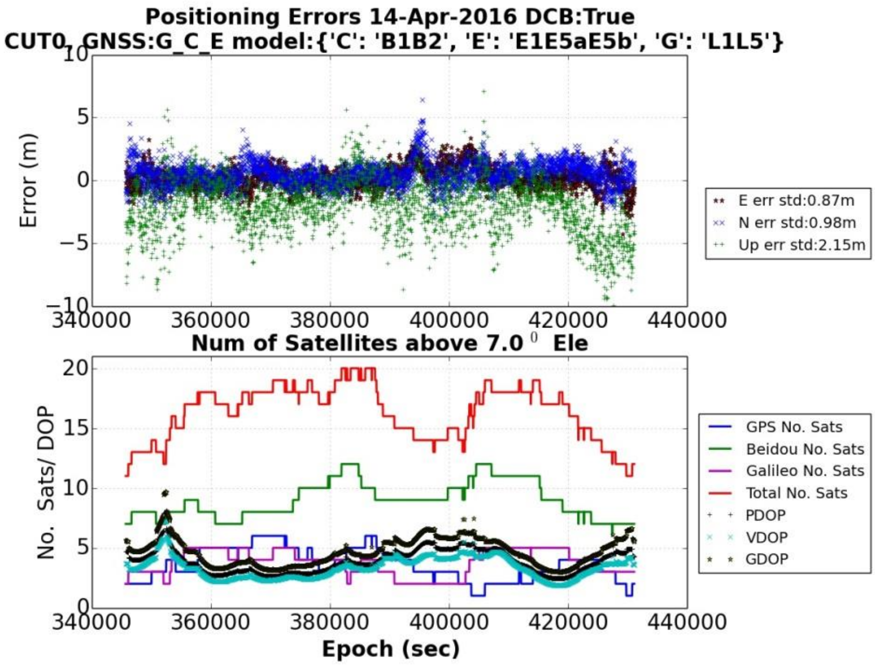

Figure 3: Positional error, satellite availability and geometry (DOPs) at station CUT0 on 14 April 2016.

Availability is measured with reference to the least number of satellites required for RAIM fault detection. A minimum of five satellites are required for fault detection and six for fault detection and isolation of a potentially erroneous satellite measurement. With multi-constellation data, at least two satellites are required from each constellation to contribute to positioning, since one satellite is dedicated to calculation of the common inter-system biases (e.g. ISTB and hardware delay). Also, since ISTB is computed relative to GPS, at least one GPS Block IIF satellite must be available at all times. Table 4 shows the percentage of time during the 24 hour period when at least five ARNS satellites were available for determination of RAIM. Beidou is available 100% of the time at all stations except at east coast Australian stations FLND and TOW2, which are just outside the Beidou coverage area. Galileo satellites have better availability in west coast stations CUT0 and KARR whereas TOW on the other hand, has relatively poor coverage for all constellations.

GNSS Constellation(s)	**Stations**					
	ALIC	**CUT0**	**NEBO**	**FLND**	**TOW2**	**KARR**
GPS	30.3	27.5	30.4	34.3	11.2	27.9
Galileo	0.0	33.0	12.0	14.5	0.0	31.6
Beidou	100	100	100	86.4	97.3	100
GPS+Beidou	100	100	100	100	100	100
GPS+Galileo	95.6	96.6	94.4	93.6	54.4	95.3
GPS+Galileo+Beidou	100	100	100	100	100	100

Table 4: Percentage availability of at least 5 ARNS satellites for determination of RAIM.

Satellite geometry is measured through DOP parameters including GDOP, PDOP and VDOP. The DOP can give approximate indication of the position error which equals $UERE \times DOP,$ where UERE is the User Equivalent Range Error. Table 5 shows the average DOP measured during the 24 hour observation period at each of the stations, as well as the percentage of time when the DOP readings were better than 5. Once again, the stations CUT0 and KARR comparatively have better availability of satellite geometry than others.

Station	**PDOP**		**VDOP**		**GDOP**	
	Mean	< 5.0 (%)	Mean	< 5.0 (%)	Mean	< 5.0 (%)
ALIC	4.59	71.08	4.13	76.44	5.59	42.82
CUT0	3.89	89.12	3.36	97.33	4.71	60.55
NEBO	4.15	86.63	3.64	91.72	5.04	66.09
FLND	3.99	90.38	3.34	97.68	4.81	66.69
TOW2	6.91	32.57	6.07	55.67	8.39	9.06
KARR	3.72	95.30	3.26	96.07	4.50	69.15

Table 5: Average DOP and percentage of time DOPs less than 5.

5.3 Integrity Monitoring

Integrity of the system is monitored using the ARAIM algorithm employing the Multiple Hypothesis Solution Separation (MHSS) method presented in Blanch et al. (2013). The use of real data in our tests allows for use of actual user range accuracy values (*URA*) received within the satellite navigation message, and determination of vertical position error (*VPE*) at stations of known positions. *VPE* is computed as the difference between the station known vertical position and the computed one from observations. Thus, we can evaluate whether *VPE* is bounded by a vertical protection level (*VPL*), which is a bound with a confidence level derived from the integrity risk requirement. Moreover, ARAIM availability is checked by testing that *VPL* is bounded by a selected vertical alert limit (*VAL*) and the availability is quantified as the fraction of time when integrity service is supported, i.e. when $VPL<VAL$. In LPV-200, *VAL* is set as 35m. If $VPE>VPL$ this is considered a misleading information event and if $VPE>VAL$ this signifies a hazardously misleading information event (El-Mowafy and Yang, 2016).

To evaluate integrity at the test sites, we compute *VPE* and *VPL* at each epoch and check that $VPE<VPL<VAL$. To compute *VPL*, we first express the linearized GNSS code measurement model as:

$$y = G\,x + G_f \nabla_f + b + \varepsilon \quad (9)$$

where *y* is the measurement vector, taken as the difference between the observed code pseudo ranges and the calculated ones from the approximate values of the coordinates; *G* is the direction cosine matrix; *x* denotes the difference between the final and approximate values of the unknown parameters, which include the three dimensional position components and receiver clock offset. *b* is a bias component and *ε* is the nominal stochastic noise. The (fault) state ∇_f is considered for possible fault modes with a characterising matrix G_f where each of its columns has a one in the index corresponding to the satellite assumed to be affected and zeros elsewhere. For a fault mode *i*, which may have one or multiple possible faulty satellites, the position estimate is:

$$\hat{x}_i = S_i\,y \quad (10)$$

where S_i is:

$$S_i = (\,(A_i\,G)^T\,W\,(A_i\,G\,)\,)^{-1}\,(A_i\,G)^T\,W \quad (11)$$

A_i is a reformed identity matrix such that the diagonal elements corresponding to the suspected faulty satellites are replaced by zero. The case of all-satellites in view (i.e. the fault-free case) is also considered where *i* is set to zero and S_i is denoted *S*.

For mode *i*, VPL_i is computed as follows:

$$VPL_i = K_{ffd,i} \times \sigma_{dV,i} + K_{md,i} \times \sigma_{v,i} + |S_{i_3}| \times bias \quad (12)$$

with $\sigma_{v,i=0} = \sqrt{e_3^T\,S^T\,Q_{URA}\,S\,e_3}$ and $\sigma_{v,i>0} = \sqrt{e_3^T\,{S_i}^T Q_{URA}\,S_i\,e_3}$. Q_{URA} is the covariance matrix of the observations using the URA values (Blanch *et al.* 2013); e_3 denotes a vector whose 3rd entry is one and zero elsewhere; K_{ffdi} and, $K_{md,i}$ are scalar factors that are used to satisfy the false alert and miss-detection probabilities and are computed from the inverse of the complement of the one-sided standard normal cumulative distribution function. $|S_{i_3}|$ is the sum of elements of the third row of $(\,S_i)$; $bias$ is the assumed maximum nominal bias used to bound potential non-zero mean error distributions for integrity evaluation. Finally, the considered value for *VPL* is the maximum VPL_i for all possible *i* modes.

Test results at stations CUT0 and TOW2 show that integrity monitoring using the triple constellation was available 100% of the time as depicted in Figure 4, which is given as a typical example for one day of data. As illustrated, the computed *VPE* was always bounded by the *VPL* and *VPL* was constantly less than *VAL*.

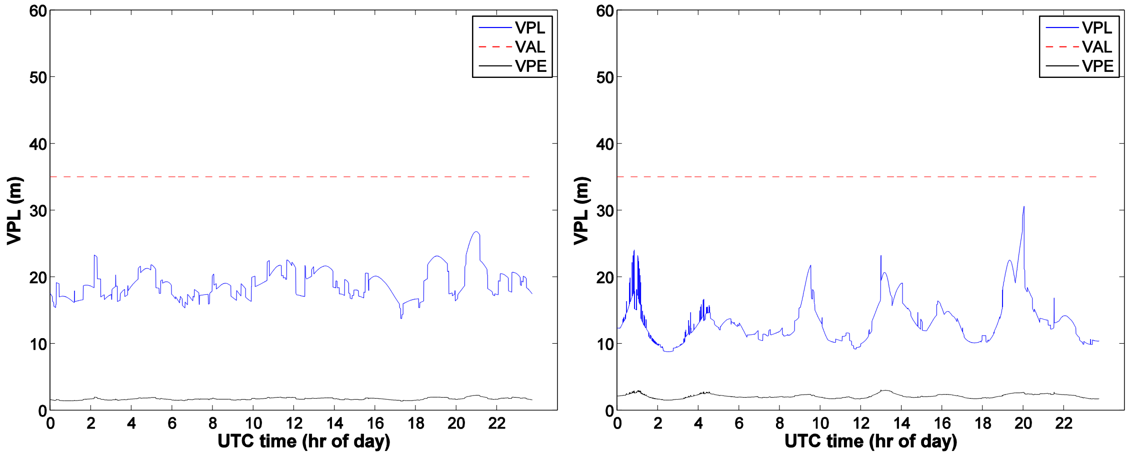

Figure 4. Integrity monitoring with *VPE*, *VPL* and *VAL* at stations CUT0 (left) and TOW2 (right) using GPS+Galileo+Beidou

7. CONCLUSIONS

This study analysed the current accuracy, availability and integrity of MFMC navigation with ARNS signals for aviation users at six sites in Australia. The GPT2 model was used to mitigate tropospheric errors, which is considered suitable for real-time aviation applications. The dual-frequency ionosphere-free combination was used for GPS and Beidou, whereas a triple frequency combination was used for Galileo. Since ARNS signals used for GPS and Galileo are not the standard signals used to generate broadcast clock corrections and broadcast DCB corrections are not presently available for aviation users, the DCB corrections from M-GEX were applied. This resulted in improvement of accuracy by 11.8%, 7.5% and 11.5% in the East, North and Up directions, respectively. The vertical positioning accuracy improved the most, by 0.3m after applying the DCB correction. Positional accuracy at west coast stations was better than other stations in central and east coast. These stations also had better availability of Galileo satellites and comparatively better satellite geometry. Beidou was available 100% of the time at all stations except east coast Australian stations FLND and TOW2, which are outside the coverage area.

Based on the results with tested data at present time, the criteria for LPV-200 horizontal positional accuracy is met easily. However the vertical accuracy achieved falls short of the required accuracy by 0.5m on average. The ARNS positioning results were dominated by the Beidou constellation, for which the IGS M-GEX recommended satellite phase antenna offset differed from calibrated values by up to 3.9m for IGSO and 1.3m for MEO satellites in z-coordinate. The situation will improve with time, as the deployment of additional ARNS satellites with improved calibrated values of Beidou antenna phase centre offsets will help to meet the LPV-200 positional accuracy requirements for future aviation users in Australia.

Tests on integrity monitoring with MFMC data for a typical day showed that integrity was available 100% of the time, where the computed VPE was always bounded by the VPL, and VPL was constantly less than VAL.

ACKNOWLEDGEMENTS

Authors acknowledge assistance received from Geoscience Australia staff for accessing RINEX V3 data for the AuScope/ ARGN sites.

REFERENCES

Allen Consulting (2013) Precise Positioning in the Aviation Sector, ACIL Allen Consulting Pty Ltd, June 2013.

Andrei CO, Chen R (2009) Assessment of time-series of troposphere zenith delays derived from the Global Data Assimilation System numerical weather model, *GPS Solutions*, 13: 109-117, DOI 10.1007/s10291-008-0104-1.

Blanch, J., et al. (2013) Critical Elements for a Multi-Constellation Advanced RAIM. *Navigation*, 60(1), 53-69.

Boehm J, Heinkelmann R, Schuh H (2007) Short Note: A Global Model of Pressure and Temperature for Geodetic Applications, *Journal of Geodesy*, 81(10): 679-683, doi:10.1007/s00190-007-0135-3.

CASA (2013) Civil Aviation Order 20.18, made under regulation 207 and 232A of the Civil Aviation Regulations 1988, Legislative Drafting Branch, Legal Services Division, Civil Aviation Safety Authority, Canberra.

Collins JP, Langley RB (1999) Nominal and Extreme Error Performance of the UNB3 Tropospheric Delay Model. Final contract report for Nav Canada Satellite Navigation Program Office, by the Geodetic Research Laboratory, Department of Geodesy and Geomatics Engineering Technical Report No. 204, University of New Brunswick, Fredericton, New Brunswick, Canada, 173 pp.

Davis JL, Herring TA, Shapiro II, Rogers AEE, Elgered G (1985) Geodesy by radio interferometry: effects of atmospheric modelling errors on estimates of baseline length, *Radio Science*, 20(6): 1593-1607.

Deo MN, El-Mowafy (2016) Triple Frequency GNSS Models for PPP with Float Ambiguity Estimation – Performance Comparison using GPS, *Survey Review*, in press.

Dilssner F, Springer T, Schönemann E, Enderle W (2014) Estimation of satellite antenna phase center corrections for BeiDou, *IGS Workshop*, Pasadena, California, USA (2014).

El-Mowafy A (2016) Pilot Evaluation of Integrating GLONASS, Galileo and Beidou with GPS in ARAIM, *Artificial Satellites*, 51(1), DOI: 10.1515/arsa-2016-0003

El-Mowafy A, Deo M, Rizos C (2016) On biases in precise point positioning with multi-constellation and multi-frequency GNSS data, *Measurement Science Technology* 27 (2016), 10pp, doi:10.1088/0957-0233/27/3/035102.

El-Mowafy A, Yang C (2015) Limited sensitivity analysis of ARAIM availability for LPV-200 over Australia using real data, *Advances in Space Research*, 57: 659–670.

GPS World (2016) Transportation: EGNOS LPV-200 Approach Implemented, *GPS World*, July 2016: 33.

Grewal MS, Petovello M, Lachapelle G (2008) What are WAAS GEO's L1 and L5 Differential biases and How Are They Estimated?, *Inside GNSS*, May/ June 2008: 22-23.

Guillermet, F (2016) Taking Precision Landing to the next level, *International Airport Review* 20(2): 23-25.

Hannan, B (2014) Next-Get Navigation, *Australian Flying*, March – April 2014: 50-55.

ICAO (2007) Aeronautical Telecommunications, in Annex 10 to the Convention on International Civil Aviation International Standards and Recommended Practices (SARPs), Volume I (Radio Navigation Aids), Montreal, Canada, July 16, 2007

IERS Conventions (2010) IERS Technical Note 36, Petit, G and Luzum, B (eds), Frankfurt am Main: Verlag des Bundesamts für Kartographie und Geodäsie, 179 pp, ISBN 3-89888-989-6.

IGS (2015) RINEX: The Receiver Independent Exchange Format Version 3.03, International GNSS Service (IGS), RINEX Working Group and Radio Technical Commission for Maritime Services Special Committee 104 (RTCM-SC104), July 14th, 2015

Kouba J (2009) A Guide to Using International GNSS Service (IGS) Products}, May 2009, Geodetic Survey Division, Natural Resources Canada, Accessed online 20 April 2010, < http://acc.igs.org/UsingIGSProductsVer21.pdf >

Lagler K, Schindelegger M, Böhm J, Krásná H, Nilsson, T (2013) GPT2: Empirical slant delay model for radio space geodetic techniques, *Geophysical Research Letters*, 40: 1069–1073.

Montenbruck O, Hauschild A and Steigenberger P (2014) Differential Code Bias Estimation using Multi-GNSS Observations and Global Ionosphere Maps, *Navigation*, 61(3): 191–201, Fall 2014.

Pajares-H (2011) Satellite Antenna Phase Centre, Accessed online 18 July 2011, <http://www.navipedia.net/index.php>

RNP PROCEDURES PAVE THE WAY, *Air Transport Action Group*, May 2013.

Rothacher M, Schmid R (2010) ANTEX: The Antenna Exchange Format, Version 1.4, Accessed online 23 March 2013, <ftp://igs.org/igscb/station/general/antex14.txt>

RTCA, 2014, *RTCA Digest Magazine*, No 217, April 2014.

Schmid R, Steigenberger P, Gendt G, Ge M, Rothacher M (2007) Generation of a consistent absolute phase center correction model for GPS receiver and satellite antennas, *Journal of Geodesy*, 81(12): 781-798.

Speidel J, Tossaint M, Wallner S, Rodriguez JA (2013) Integrity for Aviation: Comparing Future Concepts, *Inside GNSS*, July/ August 2013: 54-64.

Tuka A, El-Mowafy A (2013) Performance Evaluation of Different Troposphere Delay Models and Mapping Functions, *Measurement* 46(2): 928–937, DOI: 10.1016/j.measurement.2012.10.015.